



## SCC and Corrosion Fatigue characterization of a Ti-6Al-4V alloy in a corrosive environment – experiments and numerical models

S. Baragetti

University of Bergamo – Dept. of Engineering – viale Marconi 5, 24044 Dalmine (BG)

GITT – Centre on Innovation Management and Technology Transfer – University of Bergamo – via Salvecchio 19, 24129 Bergamo

sergio.baragetti@unibg.it

F. Villa

University of Bergamo – Dept. of Engineering – viale Marconi 5, 24044 Dalmine (BG)

francesco.villa@unibg.it

**ABSTRACT.** In the present article, a review of the complete characterization in different aggressive media of a Ti-6Al-4V titanium alloy, performed by the Structural Mechanics Laboratory of the University of Bergamo, is presented. The light alloy has been investigated in terms of corrosion fatigue, by axial fatigue testing ( $R = 0.1$ ) of smooth and notched flat dog-bone specimens in laboratory air, 3.5% wt. NaCl–water mixture and methanol–water mixture at different concentrations. The first corrosive medium reproduced a marine environment, while the latter was used as a reference aggressive environment. Results showed that a certain corrosion fatigue resistance is found in a salt water medium, while the methanol environment caused a significant drop – from 23% to 55% in terms of limiting stress reduction – of the fatigue resistance of the Ti-6Al-4V alloy, even for a solution containing 5% of methanol. A Stress Corrosion Cracking (SCC) experimental campaign at different methanol concentrations has been conducted over slightly notched dog-bone specimens ( $K_t = 1.18$ ), to characterize the corrosion resistance of the alloy under quasi-static load conditions. Finally, crack propagation models have been implemented to predict the crack propagation rates for smooth specimens, by using Paris, Walker and Kato-Deng-Inoue-Takatsu propagation formulae. The different outcomes from the forecasting numerical models were compared with experimental results, proposing modeling procedures for the numerical simulation of fatigue behavior of a Ti-6Al-4V alloy.

**KEYWORDS.** Ti6Al4V; Corrosion Fatigue; Stress Corrosion Cracking; Crack propagation; FEM.

### INTRODUCTION

The Titanium high strength-to-mass ratio Ti-6Al-4V alloy is one of the most widespread materials in advanced engineering applications, especially when high resistance is required for critical, low-weight components. For this reason, the Ti-6Al-4V alloy is hence extremely valuable for aerospace, automotive and marine high performance structural applications [1], and it has been widely applied to the biomedical sector, due to its biocompatibility and its favorable interaction with the body environment [2]. Another reason which explains the high diffusion of this particular alloy in the most demanding applications is motivated by its high resistance to a wide spectrum of corrosive environments, with respect to other Titanium based alloys, due to its inclination to form protective surface oxides [3, 4]. Sanderson et al. underlined this aspect, by concluding that the Ti-6Al-4V alloy is not susceptible to Stress Corrosion Cracking (SCC) in seawater, if considering the results of U-bend specimens [5]. In another work by Sanderson et al. [6], on the same specimen geometry and test procedures, a significant SCC effect was found for Ti-6Al-4V alloy in pure methanol



and methanol-HCl solutions. The authors observed a 30 hours fracture time for pure methanol, and a 0.3÷0.6 hours for the methanol-HCl combination. In this latter case however, water addition easily passivated the reaction. Some critical service failures were observed in the Apollo rocket Ti-6Al-4V tanks, filled with N<sub>2</sub>O<sub>4</sub> and methanol, promoting several tests in different aggressive environments to investigate on the susceptibility of this alloy. The results, found by NASA investigations presented in the works of Johnston et al. [7], and Johnson et al. [8] for static and fatigue loading of methanol filled pressurized tanks, show a high sensitivity from the methanol environment in both loading cases, as can be seen in Tab. 1. Brown [9] has collected a wide review of most of the work conducted in the late 60's on SCC of Titanium alloys and high strength steels, proposing similar conclusions. Apart from the work from NASA [7,8], which reports a direct correlation between load and the aggressive methanol environment, the other literature results [5, 6, 9, 10] are based only on static or U-bend corrosion tests, reported in terms of hours to failure, thus avoiding a direct correlation between the applied load and the corrosive environment. An example of this kind of results in a methanol-water-HCl mixture is reported in Fig. 1, from [10].

Test type	Static		Fatigue	
Environment	Load [MPa]	Time to failure [min]	Load [MPa]	Cycles to failure
Air	827	>4463 (no failure)	48-965	1385
Methanol		17		86

Table 1: Comparison between Ti-6Al-4V specimens in air and methanol environment, for static and fatigue loading, from [7]

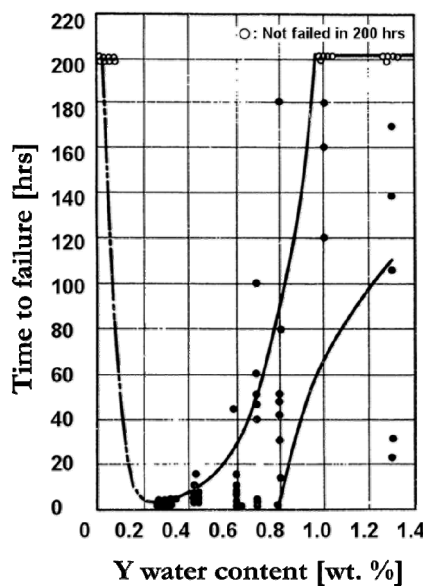


Figure 1: Time to failure for U-bend Ti-6Al-4V specimens in X wt.% Methanol – 0.17 wt.% HCl – Y wt. % Water, from [10].

It is hence mandatory to investigate further into the mechanisms which reduce the material strength in corrosive environments, since it is well known from literature that the high corrosion resistance of the Ti-6Al-4V alloy is linked to the quick oxidation of its surface, protecting the base material from the interaction with the external environment [3,4,6]. The mechanical loading, both in the tensile and fatigue cases, may compromise the effectiveness of the external oxidation passivating layer, depending also on the dynamics of the applied load, as reported in [3]. In [6], a removal of the oxide layer, both in the proximity of SCC cracks and in other regions not stress interested, was observed in the methanol-HCl solution.

A study of the mechanical behavior of Ti-6Al-4V in aggressive environments, both under quasi-static and fatigue loading is hence essential to understand the possible insurgence of SCC or corrosion fatigue behavior for this material, due to the effects that various loading conditions can impose on the alloy oxide based protection system. In the last years, the Authors research group has conducted several studies on the corrosion fatigue performances of the Ti-6Al-4V alloy in air and sea water (3.5 % wt. NaCl) [11] and on the corrosion fatigue in methanol environment at different concentrations [12]. In the present work, the most relevant results obtained by these campaigns are discussed, highlighting the effect of

the environment on different loading conditions, in terms of fatigue strength reduction. The results of an experimental campaign on the quasi-static SCC characterization of the Ti-6Al-4V alloy in methanol at different concentrations are reported, and a comparison with the fatigue data is drawn. A numerical model for the crack propagation rate for the Ti-6Al-4V alloy is proposed, in order to provide a tool to decouple the mechanical effects from the chemical driving forces.

## MATERIALS AND METHODS

The specimens for the corrosion fatigue characterization in air, 3.5 wt. % NaCl water mixture, methanol water mixture [11] and for the quasi-static testing in methanol water mixture were obtained from the same Ti-6Al-4V raw plate supply. The flat dogbone specimens were machined with a reasonable notch, according to the geometry presented in Fig. 2, in order to obtain failure in the test section with inferior loads. The test section area was of 45 mm<sup>2</sup>, while the local stress concentration factor  $K_t$  was 1.18, as obtained by a linear elastic FE simulation with plane-stress elements. The specimens were machined so that the load axis was transversal to the rolling direction of the raw Ti-6Al-4V supply plate. The chemical composition, tensile properties and successive heat treatments are reported in Tab. 2.

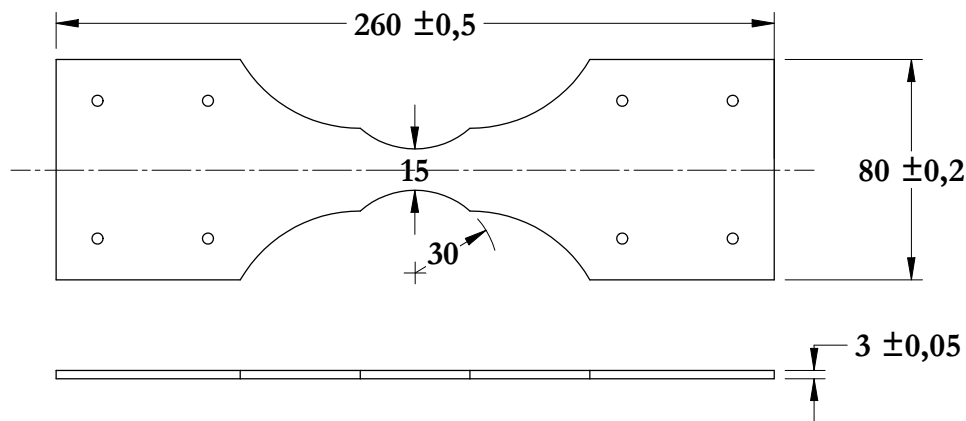


Figure 2: Specimen geometry.

Chemical Composition					
Al [%]	V [%]	Fe [%]	O [%]	C [%]	Ti [%]
5.97	4.07	0.20	0.1885	0.03	Bal.
Raw Plate Mechanical Characterization			Heat Treatments		
$R_{p,0.2}$ [MPa]	$R_m$ [MPa]	$E$ [MPa]	1. Solution treatment	2. Overaging	3. Stress relieving after machining
1'050	1'100	130'000	925 °C – 1 h	700 °C – 2 h	

Table 2: Ti-6Al-4V chemical and mechanical characteristics – including thermal treatments.

Axial fatigue loading ( $R = 0.1$ ) was imposed in the corrosion fatigue testing [11,12] in air, 3.5 wt. % NaCl water mixture and methanol water mixture at different wt. % methanol concentrations. The corrosive environment surrounded the test area of the specimens, by means of a containment device that allowed environment recirculation by means of a pump. The specimens were loaded using rolling bearing grips in order to avoid parasite bending moments during testing. A picture of the test device is reported in Fig. 3, while the tested environments are reported in Tab. 3. Step-loading technique, validated by Bellows et al. [12] and Lanning et al. [13], was adopted to obtain fatigue limits at 200'000 cycles. The 200'000 cycles number was selected by observing the S-N fatigue data of Sadananda et al. [14], where it is found that the  $R = -1$  specimens reach a constant limit, and the steepness of the  $R = 0.1$  test results decreases significantly. Specimens were tested at a given maximum stress, and if they reached the end of the cycles block without a failure, the load was increased and the test was restarted. The final fatigue limit was obtained by a linear interpolation between the failed load block and the previous not failed block, according to the formula:

$$\sigma_{FL,N} = \sigma_{pb} + \frac{N_f}{N} (\sigma_{fb} - \sigma_{pb})$$

where  $\sigma_{FL,N}$  is the fatigue strength limit at  $N$  cycles,  $\sigma_{fb}$  is the applied load during the failed cycle block,  $N_f$  is the number of cycles at which failure is reached during the failed block, and  $\sigma_{pb}$  is the applied load during the previous, not failed block. Two specimens were tested for every environmental configuration, in order to confirm the results.

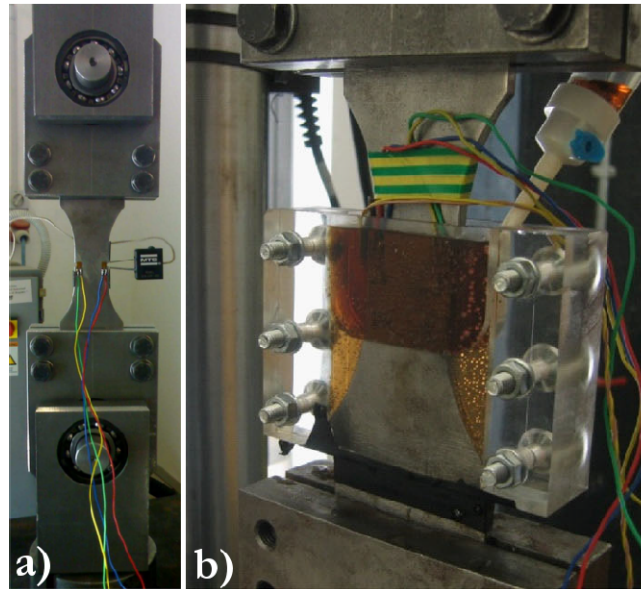


Figure 3: Corrosion fatigue test setup: (a) Specimen mounted on hinge grips to avoid parasite bending; (b) Aggressive environment containment system. Adapted from [11].

Test type	Fatigue
Environments	Air, 3.5%wt NaCl-water solution, Methanol-water solution
Methanol wt. % conc. tested	5%, 25%, 50%, 95%

Table 3: Test environments for corrosion fatigue testing, from [11].

A quasi-static stress corrosion campaign was conducted on the same specimen geometry and material, in order to decouple the mechanical effects from the chemical driving forces, quantifying the contribution of the different load application. The tests were performed in air and in methanol environment, using the same methanol concentrations adopted in the fatigue tests, as well as other intermediate concentrations to improve the resolution and confidence on the obtained results. The environmental test conditions are reported for both corrosion fatigue and quasi-static SCC tests in Tab. 4, while the test setup for the quasi-static campaign is depicted in Fig. 4. The specimens were loaded by means of a threaded rod tensile system, and mounted on similar rolling bearing hinge grips to avoid parasite moments. To control the effectiveness of the procedure, strain-gages were mounted on the front and rear faces of each specimen, and correlated by means of FE analysis to the actual throat stress. A direct placement of the strain gages in the test section was avoided, since it would have required to remove the oxide layer, thus modifying the test conditions. The applied load was measured by means of a load cell applied on the rod. The load was augmented every hour by a value of 5 MPa. The mean deformation velocity was hence calculated as

$$\dot{\epsilon} = \frac{\Delta\sigma}{E\Delta t} = 1.23 \cdot 10^{-8} \left[ s^{-1} \right]$$

The aggressive environment was placed in a containment system near the specimen test section, granting continuous full immersion of the specimen throat, as in the corrosion fatigue tests. Methanol was added during the tests, and removed whenever the tests were paused.

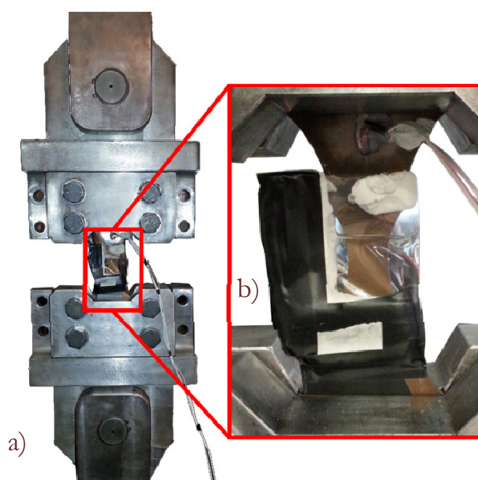


Figure 4: Experimental setup for the quasi static SCC tests: (a) Specimen mounted on hinge grips; (b) Methanol containment system and applied strain gages.

Test type	Static
Environments	Air, Methanol-water solution
Methanol wt. % conc. tested	25%, 50%, 75%, 85%, 90%, 92.5%, 95%, 97.5%, 99.8% (maximum purity)

Table 4: Test environments for quasi-static SCC testing.

## EXPERIMENTAL RESULTS

### Corrosion fatigue data

The corrosion fatigue  $\sigma_{max}$  data, obtained by the results of [11] by using the Haigh diagram with  $R = 0.1$ , are presented in Fig. 5, showing the effect of aggressive environment compared with testing in laboratory air. The cycles number adopted for the step-loading technique was selected at 200'000. The data related to fatigue testing in methanol, compared with the results for air and 3.5% wt. NaCl-water solution, identify a dramatic decrease of fatigue strength even from the least concentrated (5%) methanol solution. The detrimental effect of methanol increases then with concentration. The effect of mechanical loading in this case seems to improve the corrosion effects even for very light methanol concentrations: a 24% maximum stress loss is detected for the 5% methanol solution, against a 56% loss for the 95% methanol concentration. These data indicate that, with respect to the U-bend Ti-6Al-4V specimens, which showed a marked SCC behavior only for very high methanol concentrations [10], there is a strong influence of the mechanical stress effects in the corrosion fatigue process.

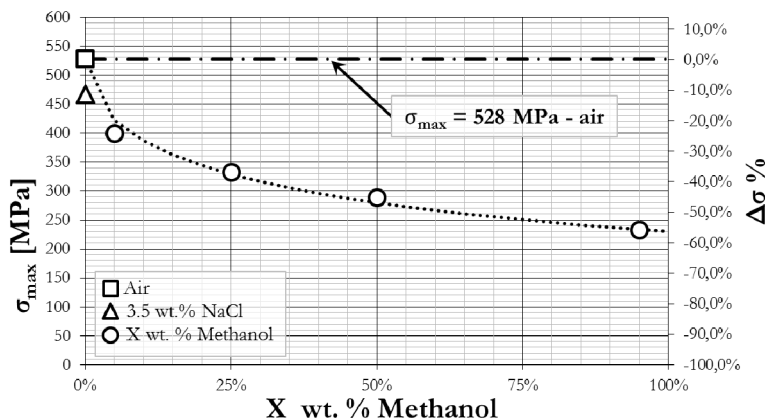


Figure 5: Corrosion fatigue test results for air, 3.5 % wt. NaCl water mixture and different wt. % Methanol water mixture at 200'000 cycles, adapted from [11].

### Quasi-static SCC data

The results of the quasi-static testing campaign in air and methanol at different concentrations are reported in Fig. 6.

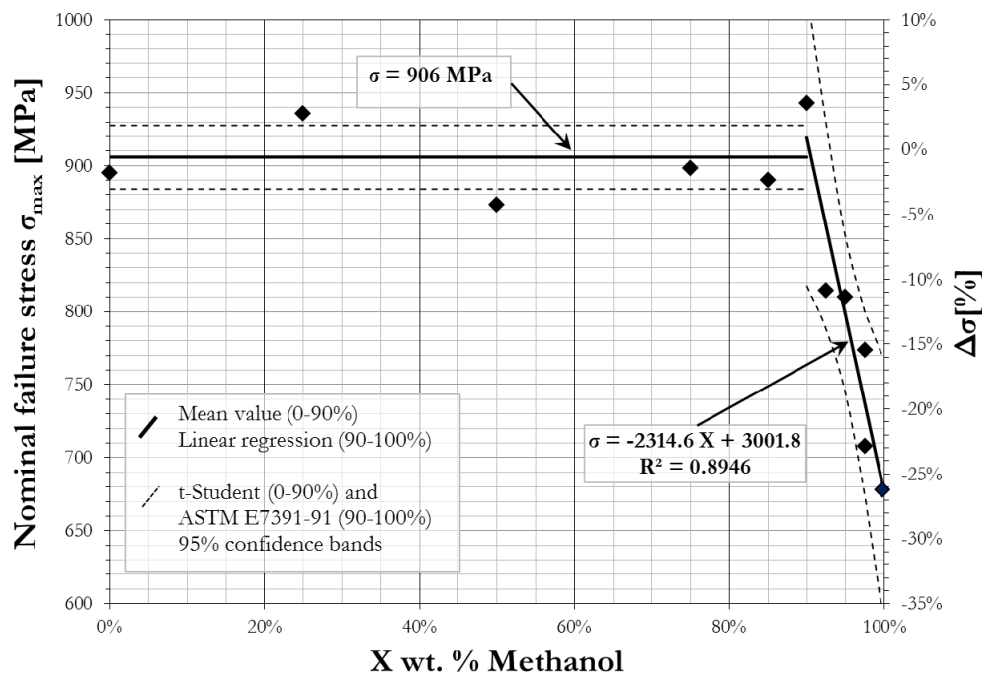


Figure 6: Quasi-static experimental data and interpolations with confidence bands for Ti-6Al-4V specimens tested in air and methanol water solution at different concentrations, in terms of maximum nominal stress in the test section.

The quasi-static results indicate that the SCC behavior show a reduction of the failure stress starting from a 90% wt. methanol concentration in water. The overall drop is limited for pure methanol, with a -25% in terms of nominal stress applied to the test section. However a marked methanol effect is recognizable even for a 92.5 % methanol concentration, if compared to higher results from literature [10].

### Comparison between Corrosion Fatigue and Quasi-static SCC data

The results in terms of maximum stress drop in function of methanol concentration have been extracted from the experimental data presented in this work, and compared between the fatigue and quasi-static tests. The chemical driving forces in the two different cases have been highlighted by extracting the difference from the mechanical failure stress, according to the following relations:

$$\sigma_{chem, QS} = \sigma_{mech, QS} - \sigma_{QS}(X_{met})$$

$$\sigma_{chem, F} = \sigma_{mech, F} - \sigma_F(X_{met})$$

The direct comparison is presented in Fig. 7.

Fig. 7 remarks the difference in terms of the material strength behavior in an aggressive methanolic media for the Ti-6Al-4V alloy for different loading conditions. It must be recognized that a dynamic loading causes an onset of corrosive effect even from mild methanol concentrations, while a methanol concentration over 90% is needed in a quasi-static SCC condition. The different loading conditions may affect the protective role of the surface oxide of the alloy showed in [3,4,6]. In particular, fatigue loading may induce premature cracking of the substrate oxide, resulting in an enhanced susceptibility of the material to the external environment, while quasi-static conditions require higher methanol concentrations to damage the external film. Further analyses at different loading conditions, number of cycles and frequencies are needed in order to evaluate the mechanical loading effects on the corrosion protection characteristics of the Ti-6Al-4V alloy.

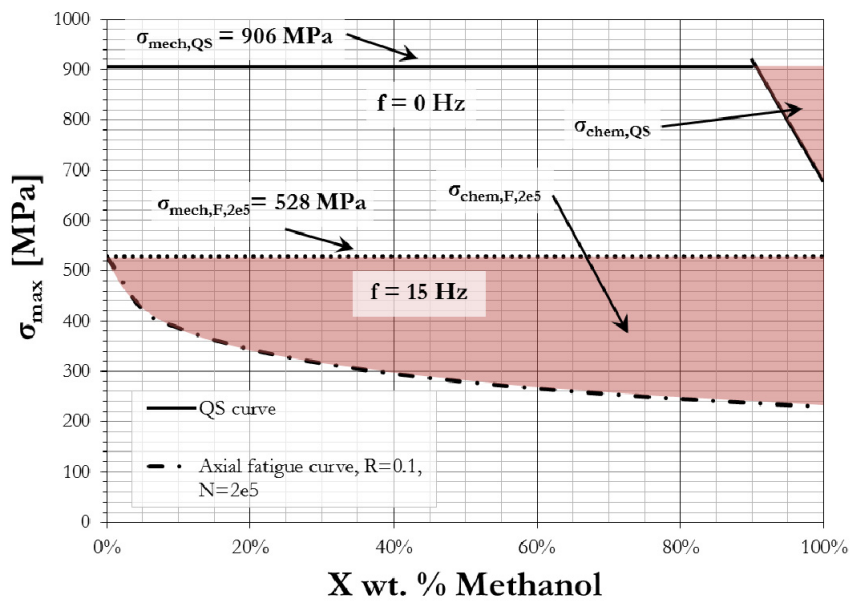


Figure 7: Corrosion effects in terms of mechanical and chemical stress contributions in different load conditions.

## NUMERICAL MODELS

### *Elastic stress intensity factor field*

In order to deepen the investigation on the mechanical effects involved in the process, a FE simulation procedure was developed to predict the fatigue crack propagation rate for a Ti-6Al-4V alloy. The model was based on the experimental  $da/dN - \Delta K$  results obtained by Lee et al. [15] for the same alloy.

The FE model of a flat smooth fatigue specimen was realized using linear plane stress elements, the geometry being compatible with the one reported in [16]. The crack was modeled in the throat section starting from an initial length of 5  $\mu\text{m}$ , and propagated by a finite step  $\Delta a$  until the value of  $K_{IC}$  was obtained. The value of the first mode stress intensity factor field  $K_I$  is hence obtained from the half crack tip opening displacement in the longitudinal, tensile direction  $u_y$ , by using the following relations [17]:

$$K_I(r, \vartheta) = \frac{E}{1+\nu} \sqrt{\frac{2\pi}{r}} \frac{u}{f(\vartheta)}$$

$$f(\vartheta) = \sin\left(\frac{\vartheta}{2}\right) \left[ \kappa + 1 - 2\cos^2\left(\frac{\vartheta}{2}\right) \right]$$

with  $\kappa = 3 - 4\nu$  for plane strain and  $\kappa = (3 - \nu)/(1 + \nu)$  for plane stress state. The presented  $K_I$  model is valid in the elastic field of the material. In the presence of a sharp notch, the stresses may rise above the yielding stress. However, according to Milella [18], if the plastic zone is inferior to 1 mm, small scale yielding (SSY) conditions are reached, and the linear stress field relations can be used for fatigue crack propagation. Due to the very high yielding stress of the considered Ti-6Al-4V alloy, a SSY condition is very likely to be reached in our case, and the [17] relations are thus adopted.

To obtain  $K_I$ , a value of  $E$  equal to 113000 MPa and a  $\nu$  of 0.342 for the Ti-6Al-4V alloy were adopted, and a plane stress state was considered, coherently with the FE modeling and with the actual load situation. The vertical displacement  $u_y$ , as well as the coordinates  $r$  and  $\theta$  have been taken from the first and second node away from the crack tip, and the corresponding value of the applied  $\Delta K$  was obtained by extrapolating linearly the  $K_I$  value to the crack tip. The adopted coordinate system and an example of the stress distribution map for the smooth specimen, at a crack propagation depth of 50  $\mu\text{m}$ , are displayed in Fig. 8. The applied nominal tensile load was of 548 MPa, while the measured stress concentration factor  $K_t$  in the linear elastic field, prior to the crack introduction, was of 1.18.

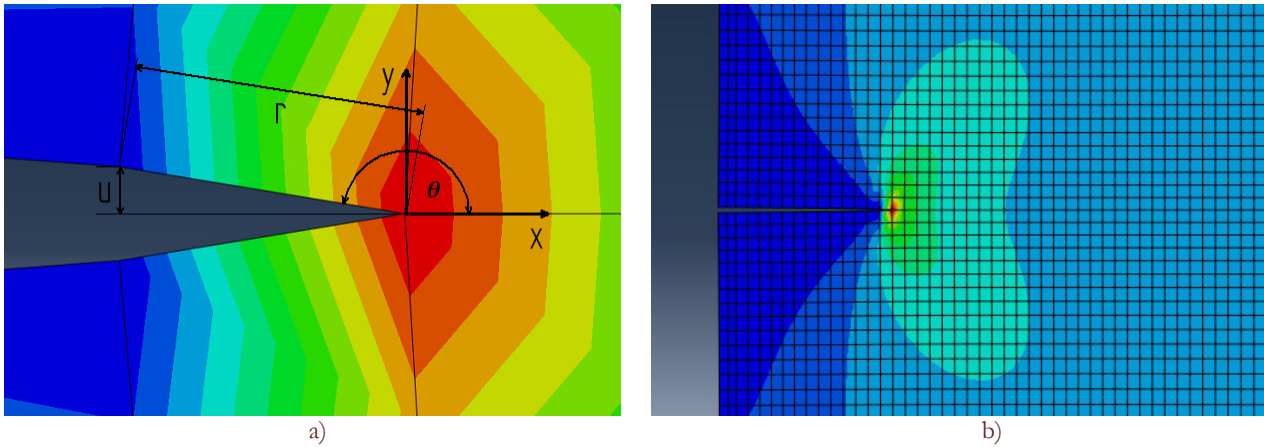


Figure 8: FE model for the crack propagation model: (a) Coordinate system for the elastic stress intensity factor field calculation; (b)  $\sigma_y$  stress field around the crack tip for a propagation depth of 50  $\mu\text{m}$ .

### Crack propagation models

Once the model for the determination of the  $K_I$  field has been defined, a propagation law for the crack front is needed. In the present work, three models have been applied to the case. The models of Paris [17], Walker [19] and Kato et al. [20] have been proposed and applied to the obtained stress intensity factors for the two considered FE models.

The first, most common adopted model for the crack propagation growth rate is the Paris model [17], which simply assumes a power-law dependence of the growth rate from the stress intensity factor, thus describing only the stable propagation rate. Paris' law takes the form:

$$\frac{da}{dN} = C (\Delta K)^n$$

where  $\Delta K$  is the applied stress intensity factor, defined as  $\Delta K = (1 - R)K_{max}$  [15], with  $K_{max}$  obtained from the FE model. For the Ti-6Al-4V alloy, the Paris constants are assumed as  $C = 3.8 \cdot 10^{-8} [(\text{mm}/\text{cycle}) / (\text{MPa}\sqrt{\text{m}})^n]$  and  $n = 3.11$ , from [21]. The Paris model reconstructs the stable propagation region as a straight line in a log-log diagram, not considering the effect of the load ratio  $R$  as well as other properties of the material.

A more sophisticated relation is proposed in the Walker model [19], which takes into account the effect of the load ratio, with the empirical law:

$$\frac{da}{dN} = \frac{C_1}{(1-R)^{m_1(1-\gamma)}} \Delta K^{m_1}$$

where  $C_1$  and  $m_1$  are the same as Paris' law,  $\gamma$  is an additional parameter which gives an offset to the log-log stable propagation rate curve.

A more detailed model is the one proposed for case carburized steel spur gears from Kato et al. [20], which includes a relation to obtain the threshold crack propagation stress intensity  $\Delta K_{th}$ , as well as a description of both the quasi-static crack propagation region and the stable crack growth propagation region, thus defining a transition stress intensity factor  $K_C$ . The model consists in two crack propagation rate laws, one for the initial and the other for the stable growth region:

$$\left\{ \begin{array}{l} \frac{da}{dN} = \frac{C}{(1-\rho^n)} (\Delta K^n - \Delta K_{th}^n) \quad \text{for } \Delta K_{th} < \Delta K < K_C \\ \frac{da}{dN} = \frac{C}{(1-\rho^n)} \left( \frac{\Delta K^n \Delta K_{IC}^n}{\Delta K_{IC}^n - \Delta K^n} \right) \quad \text{for } K_C < \Delta K < K_{IC} \end{array} \right.$$

with

$$\rho = \frac{\Delta K_{th}}{K_{IC}}, \quad K_C = (\Delta K_{th} K_{IC})^{1/2}$$

The Authors of [20] propose an experimental correlation between the threshold  $\Delta K_{th}$  value, the model parameters  $C$  and  $n$  and the fracture toughness  $K_{IC}$  which takes into account the material HV hardness. The model was developed to describe case carburized steel gears with hardness profiles variable with the depth, while in our case a constant measured hardness of 350 HV was used. The experimental relations are:

$$\Delta K_{th} = 2.45 + 3.41 \cdot 10^{-3} H = 3.64 \text{ MPa}\sqrt{m}$$

$$K_{IC} = 141 - 1.64 \cdot 10^{-1} H = 83.6 \text{ MPa}\sqrt{m}$$

$$n = 4.31 - 8.66 \cdot 10^{-3} H + 1.17 \cdot 10^{-5} H^2$$

$$\log(C) = -10.0 + 1.09 \cdot 10^{-2} H - 1.40 \cdot 10^{-5} H^2$$

### Numerical results

The three different models have been adopted to reconstruct the  $da/dN - \Delta K$  curve for a  $R = 0.1$ , to be compared directly with the data obtained by *Lee et al.* for the same alloy and load conditions [15], as shown in Fig. 9. The stress data of the FE model have been inserted in the three models at different discrete intervals of  $a$ , obtaining a  $da/dN$  curve covering the whole interval from  $\Delta K_{th}$  to  $K_{IC}$ , as taken directly from the *Kato et al.* model [20]. Since the value obtained by the model proposed in [20], *i.e.*  $K_{IC} = 83.6 \text{ MPa}\sqrt{m}$ , is quite high for a Ti-6Al-4V alloy, a comparison with literature data for STA annealed Ti-6Al-4V [22] is also shown, the proposed value being  $K_{IC,Lit} = 43 \text{ MPa}\sqrt{m}$ .

From the results, it can be seen that the Paris model provides a suitable description of the constant growth rate region, although the Walker model reaches a better correlation. The Kato model shows a good resemblance with the material behavior in the proximity of the threshold value, describing correctly the initial growth phase, in contrast with the other two models. The threshold result obtained by this model has proved to be in good correspondence with the experimental data, as in Fig. 9.

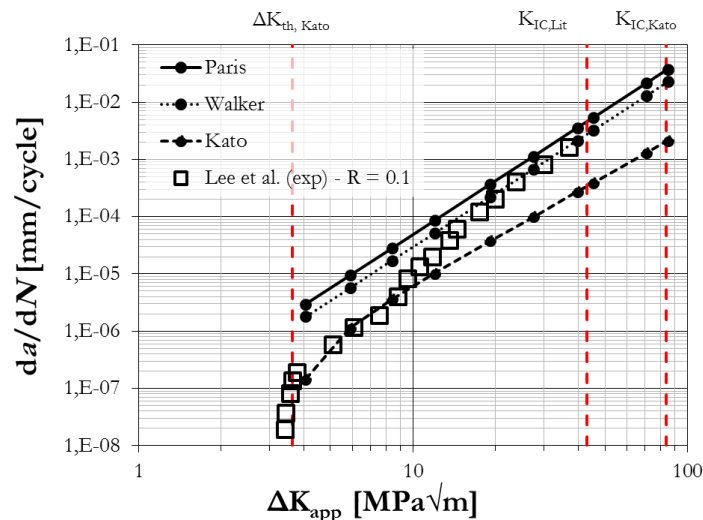


Figure 9: Comparison between the proposed propagation models of Paris, Walker, Kato, based on actual FE results, and the experimental data from Lee et al. [15]. Each solid point represents the  $da/dN$  value obtained by a single FE simulation.

### CONCLUSIONS

In the present work, an overview of the recent results of the Authors research group on the corrosion behavior of the Ti-6Al-4V alloy in different loading conditions and various aggressive environment conditions is presented. The considered alloy has shown good corrosion fatigue resistance properties in a 3.5 wt.% NaCl-water mixture, while a significant drop of fatigue performance (-56%  $\sigma_{max}$  loss) is found at high methanol concentrations. The corrosion fatigue  $\sigma_{max}$  drop persisted, even if with reduced intensity (-24%), for the minimum 5 wt.% methanol concentration. A different behavior was observed for quasi-static SCC tests, where the effect of the aggressive solution was not observed below a 92.5 wt. % concentration of methanol in water. The maximum quasi-static drop for the reagent grade ( $\geq 99.8$  wt. %) was observed at 92.5 wt. % concentration of methanol in water.



methanol maximum concentration observed in this case was of -25% in terms of nominal applied stress. A direct dependence of the degradation of the mechanical characteristics of the alloy from the loading conditions was found. This dependence may be explained by the different damage mechanisms occurring on the protective oxides on the alloy surface. The chemical driving forces have been decoupled from the mechanical contribution in air, and an environmental effect in terms of chemical stresses  $\sigma_{\text{chem}}$  has been isolated for different loading conditions. Finally, a FE model to describe the mechanical effects in terms of crack propagation for smooth fatigue specimens has been developed, by comparing different crack propagation laws to literature data. This model will be useful to improve the study of the mechanical effects involved in the corrosion fatigue process, by providing a chemical free simulation of the crack advancement, to be compared with experimental results in air and aggressive environments.

## ACKNOWLEDGMENTS

The Authors wish to thank Eng. Marco Giustinoni and Mr. Marco Ceresoli for the help in the test setup and in the FE models realization.

## REFERENCES

- [1] Lütjering, G., Williams, J.C., Titanium, second ed., Springer, Berlin (2007).
- [2] Dimah, M.K., Devesa Albeza, F., Amigó Borrás, V., Igual Muñoz, A., Study of the biotribocorrosion behavior of titanium biomedical alloys in simulated body fluids by electrochemical techniques, *Wear*, 294–295 (2012) 409–418.
- [3] Codaro, E.N., Nakazato, R.Z., Horovistiz, A.L., Ribeiro, L.M.F., Ribeiro, R.B., Hein, L.R.O., An image analysis study of pit formation on Ti-6Al-4V, *Mater. Sci. Eng. A*, 341 (2003) 202–210.
- [4] Gurrappa, I., Characterization of titanium alloy Ti-6Al-4V for chemical, marine and industrial applications, *Mater. Charact.*, 51 (2003) 131–139.
- [5] Sanderson, G., Powell, D.T., Scully, J.C., The Stress-Corrosion Cracking of Ti Alloys in Aqueous Chloride Solutions at Room Temperature, *Corros. Sci.*, 8 (1968) 473–481.
- [6] Sanderson, G., Scully, J.C., The Stress-Corrosion Cracking of Ti Alloys in Methanolic Solutions, *Corros. Sci.*, 8 (1968) 541–548.
- [7] Johnston, R.L., Johnson, R.E., Ecord G.M., Castner W.L., Stress-Corrosion Cracking of Ti-6Al-4V Alloy in Methanol, NASA Technical Note TN D-3868 (1967).
- [8] Johnson, R.E., Nasa Experiences with- Ti-6Al-4V In Methanol, DMIC Memorandum 228 (1967) 2–7.
- [9] Brown, B.F., Stress-Corrosion Cracking in High Strength Steels and in Titanium and Aluminum Alloys, first ed., Naval Research Laboratory, Washington (1972).
- [10] Chen, C.M., Kirkpatrick H.B., Gegel H.L., Stress Corrosion Cracking of Titanium Alloys in Methanolic and Other Media, Technical Report AFML-TR-71-232, USAF Materials Laboratory, Wright-Patterson AFB (1972).
- [11] Baragetti, S., Corrosion fatigue behaviour of Ti-6Al-4V in methanol environment, *Surf. Interface Anal.*, 45 (2013) 1654–1658.
- [12] Bellows, R.S., Muju, S., Nicholas, T., Validation of the step test method for generating Haigh diagrams for Ti-6Al-4V, *Int. J. Fatigue*, 21 (1999) 687–697.
- [13] Lanning, D.B., Haritos, G.K., Nicholas, T., Influence of stress state on high cycle fatigue of notched Ti-6Al-4V specimens, *Int. J. Fatigue*, 21 (1999) S87–S95.
- [14] Sadananda, K., Sarkar, S., Kujawski, D., Vasudevan, A.K., A two-parameter analysis of S-N fatigue life using  $\Delta\sigma$  and  $\sigma_{\text{max}}$ , *Int. J. Fatigue* 31 (2009) 1648–1659.
- [15] Lee, E.U., Vasudevan, A.K., Sadananda, K., Effects of various environments on fatigue crack growth in Laser formed and IM Ti-6Al-4V alloys, *Int. J. Fatigue* 27 (2005) 1597–1607.
- [16] Baragetti, S., Notch Corrosion Fatigue Behavior of Ti-6Al-4V, *Materials* 7 (2014) 4349–4366.
- [17] Anderson, T.L., Fracture Mechanics, third ed., Taylor & Francis, Boca Raton (2005).
- [18] Milella, P.P., Fatigue and Corrosion in Metals, first ed., Springer Verlag Italia, Milan (2013).
- [19] Beden, S.M., Abdullah S., Ariffin A.K., Review of Fatigue Crack Propagation Models for Metallic Components, *Eur. J. Sci. Res.*, 3 (2009), 364–397.



- [20] Kato, M., Deng, G., Inoue, K., Takatsu, N., Evaluation of the Strength of Carburized Spur Gear Teeth Based on Fracture Mechanics, *JSME Int. J., Ser. C*, 36(2) (1993) 233–240.
- [21] Carpinteri, A., Paggi, M., Self-similarity and crack growth instability in the correlation between the Paris' constants, *Eng. Fract. Mech.*, 74 (2007) 1041–1053.
- [22] MatWeb: [www.matweb.com](http://www.matweb.com), (2014).